© 2019. Published by The Company of Biologists Ltd | Development (2019) 146, dev177139. doi:10.1242/dev.177139

STEM CELLS AND REGENERATION

RESEARCH ARTICLE

# Regulation of the ERK signalling pathway in the developing mouse blastocyst

**Takuya Azami[1,*], Cécilia Bassalert[2,*], Nicolas Allègre[2], Lorena Valverde Estrella[2], Pierre Pouchin[2], Masatsugu Ema[1,3,‡] and Claire Chazaud[2,‡]**

## ABSTRACT

Activation of the ERK signalling pathway is essential for the differentiation of the inner cell mass (ICM) during mouse preimplantation development. We show here that ERK phosphorylation occurs in ICM precursor cells, in differentiated primitive endoderm (PrE) cells as well as in the mature, formative state epiblast (Epi). We further show that DUSP4 and ETV5, factors often involved in negative-feedback loops of the FGF pathway, are differently regulated. Whereas DUSP4 presence clearly depends on ERK phosphorylation in PrE cells, ETV5 localises mainly to Epi cells. Unexpectedly, ETV5 accumulation does not depend on direct activation by ERK but requires NANOG activity. Indeed ETV5, like *Fgf4* expression, is not present in *Nanog* mutant embryos. Our results lead us to propose that in pluripotent early Epi cells, NANOG induces the expression of both *Fgf4* and *Etv5* to enable the differentiation of neighbouring cells into the PrE while protecting the Epi identity from autocrine signalling.

**KEY WORDS: Mouse, Blastocyst, Cell differentiation**

## INTRODUCTION

Signalling between cells is crucial for tissue differentiation and is required during the earliest steps of embryo differentiation. During mouse preimplantation, three cell lineages are produced from two successive differentiation events. The first differentiation between outer and inner cells is essentially driven by the Hippo signalling pathway leading to the production of trophectoderm (TE) and inner cell mass (ICM) cells, respectively (Menchero et al., 2016; Nishioka et al., 2009). During blastocyst formation around embryonic day (E)3.5, epiblast (Epi) and primitive endoderm (PrE) cells appear within the ICM in a 'salt-and-pepper' pattern evidenced by the reciprocal and complementary expression pattern of the transcription factors NANOG and GATA6 (Chazaud et al., 2006; Guo et al., 2010; Kurimoto et al., 2006; Plusa et al., 2008). Numerous experiments have shown that the FGF/ERK pathway balances this binary cell fate, as high signals induce cells into PrE whereas blocking the pathway leads ICM cells toward an Epi fate (Bessonnard et al., 2017; Chazaud et al., 2006; Feldman et al., 1995; Kang et al., 2013, 2017; Krawchuk et al., 2013; Molotkov et al., 2017; Nichols et al., 2009; Ohnishi et al., 2014; Saiz et al., 2016; Yamanaka et al., 2010). Interestingly, FGF4, the sole FGF ligand detected at this stage (Ohnishi et al., 2014), is transcribed and secreted from Epi cells only (Frankenberg et al., 2011; Guo et al., 2010; Kurimoto et al., 2006; Ohnishi et al., 2014), converting neighbouring cells into PrE, illustrated by expression of the PrE markers SOX17 and GATA4 (Frankenberg et al., 2011). *Fgfr2* is specifically expressed in PrE cells (Guo et al., 2010; Kurimoto et al., 2006; Ohnishi et al., 2014); however, *Fgfr1*, which is equally expressed in Epi and PrE cells, is the initial and main receptor transducing the FGF activity required for PrE specification (Kang et al., 2017; Molotkov et al., 2017).

Despite the increasing data demonstrating the importance of the FGF/ERK pathway during blastocyst development, expression of activated phosphorylated ERK (pERK) has not been described yet. FGF target genes have been recently examined using *Fgfr1/2* mutant embryos (Kang et al., 2017). Although *Dusp4* is preferentially detected in PrE cells, as would be expected with a pERK activity required in this cell type, other genes, such as *Etv4/5*, which are ETS-related factors, and *Sprouty* (*Spry*)*2/4*, which are negative regulators of the pathway, are expressed in both cell types (Kang et al., 2017). It was then proposed that a low pERK activity could be present also in Epi cells, where it would activate negative-feedback loops involving ETVs and SPRYs to protect the Epi state (Kang et al., 2017).

Here, we show that ERK phosphorylation begins around E3.0-E3.25 days, concomitant with the initiation of Epi/PrE specification, and is present in ICM progenitor or PrE cells. This activation of the pathway is respectively increased and lost in *Klf5* and *Fgf4* mutants, which is in accordance with the described phenotypes (Azami et al., 2017; Kang et al., 2013; Krawchuk et al., 2013; Ohnishi et al., 2014). We also found that DUSP4 accumulation tightly follows pERK activity, whereas, surprisingly, ETV5 accumulation is not directly regulated by the MAPK pathway but clearly depends on NANOG expression. Our results lead to a novel model of FGF/ERK regulation in the preimplantation embryo.

## RESULTS

### Detection of pERK in preimplantation embryos

The FGF/ERK signalling pathway plays pivotal roles in the segregation of Epi and PrE cells, yet there is currently no reliable method to detect pERK during preimplantation stages, thereby hampering the understanding of how pERK regulates the fundamental process of preimplantation development. We have developed two new methods to detect ERK phosphorylation that are sufficiently sensitive to detect signals in preimplantation embryos. Briefly, to preserve the integrity of the phosphate conjugate we add phosphatase inhibitors during the fixation step and permeabilisation

[1]Department of Stem Cells and Human Disease Models, Research Center for Animal Life Science, Shiga University of Medical Science, Seta, Tsukinowa-cho, Otsu, Shiga 520-2192, Japan. [2]GReD Laboratory, Université Clermont Auvergne, CNRS, Inserm, Faculté de Médecine, CRBC, F-63000 Clermont-Ferrand, France. [3]Institute for the Advanced Study of Human Biology (ASHBi), Kyoto University Institute for Advanced Study 606-8501, Japan.
*These authors contributed equally to this work

‡Authors for correspondence (mema@belle.shiga-med.ac.jp; claire.chazaud@uca.fr)

M.E., 0000-0003-0645-6183; C.C., 0000-0002-6748-6039

**Received 26 February 2019; Accepted 11 July 2019**

Development (2019) 146, dev177139. doi:10.1242/dev.177139

is carried out either with Triton X-100 or proteinase K (see Materials and Methods). Two working methods (Fig. S1A) provide alternative solutions to observe other labelling in co-staining experiments. Phosphorylation of ERK is evident in the cytoplasm and mitotic nuclei can retain a strong labelling (Fig. S1B,C) (Shapiro et al., 1998). Cytoplasmic localisation of pERK has been reported previously in early mouse embryos (Corson et al., 2003) and, interestingly, it was suggested that this subcellular labelling is reminiscent of differentiation rather than proliferation events (Marenda et al., 2006; Michailovici et al., 2014).

The presence of exogenous FGF has been shown to increase the number of PrE cells (Yamanaka et al., 2010); we found that culturing embryos with recombinant FGF between E2.5 and E3.75 increased the number of pERK-labelled cells as well as its signal intensity, with almost all ICM cells exhibiting an elevated pERK signal compared with the control (Fig. S2A). Interestingly, an increase of pERK staining could be observed after only 10 min of FGF treatment (Fig. S2B). To further validate these techniques, we collected E2.5 embryos and cultured them until E3.75 with MEK or FGFR+MEK inhibitors, which block the pathway upstream of ERK phosphorylation (Nichols et al., 2009; Yamanaka et al., 2010). The pERK signal was totally downregulated in the presence of inhibitors (Fig. S2C), confirming the specificity of our methods. Thus, we established for the first time two protocols to detect pERK during preimplantation development.

### ERK phosphorylation begins during blastocyst formation

We analysed ERK phosphorylation during preimplantation development from the one-cell stage, thus before the reported *Fgf4* expression that starts in a subset of the inner cells between E3.0 and E3.25 (Guo et al., 2010; Ohnishi et al., 2014). Cells expressing pERK were first detected around E3.0 (Fig. 1A). The number of labelled cells increased with time, exhibiting graded pERK levels (Fig. 1A-C). A few TE cells were marked (Fig. S1B) and this is

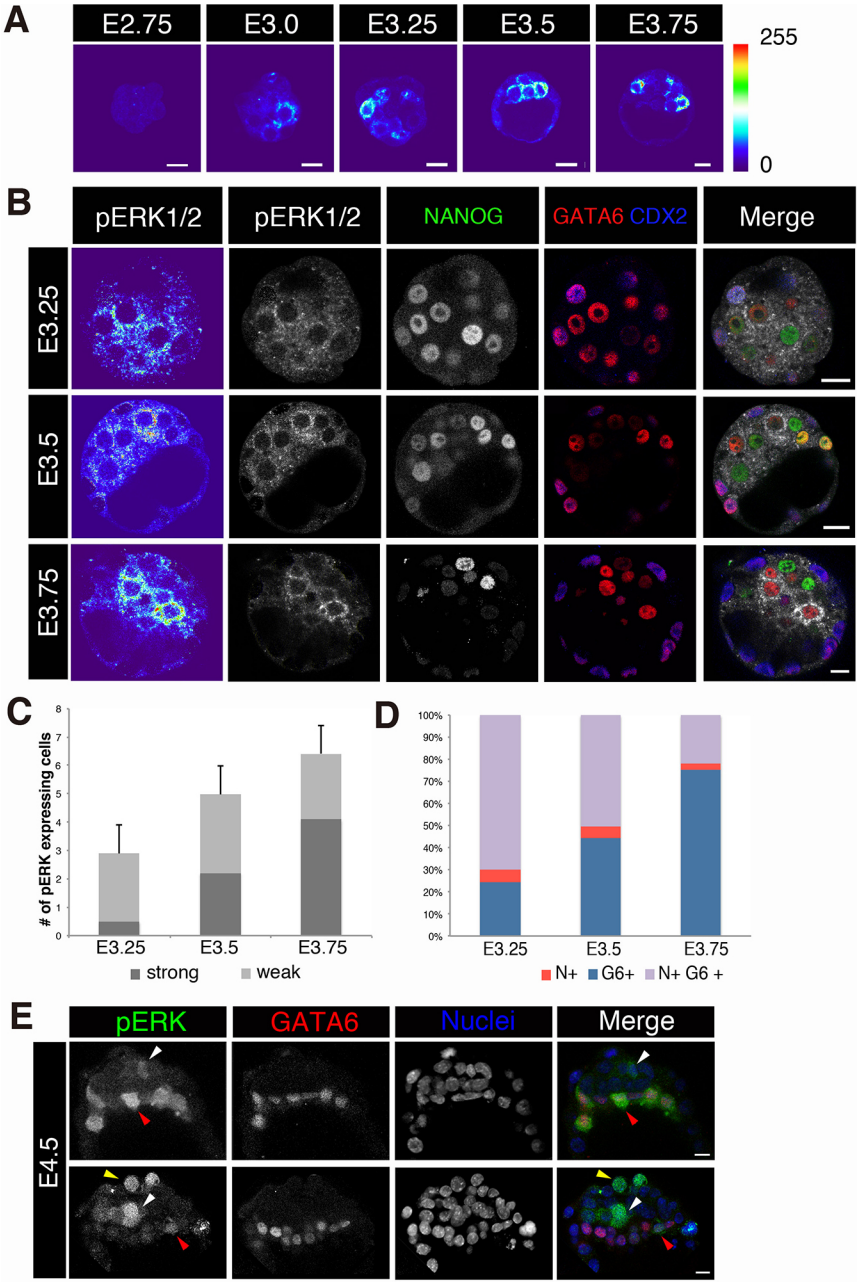


**Fig. 1. ERK phosphorylation during Epi/PrE specification.** (A) Immunolocalisation of pERK from E2.75 to E3.75. Colour scale indicates signal intensity. (B) Immunostaining for pERK, CDX2, NANOG and GATA6 immunostaining from E3.25 to E3.75. (C) Number of pERK-labelled cells in the ICM at E3.25 ($n$=29 embryos), E3.5 ($n$=30) and E3.75 ($n$=30). Data are represented as mean±s.e.m. (D) Distribution of the ICM pERK-labelled cells shown in B between NANOG$^{+}$/GATA6$^{-}$ (N+), NANOG$^{-}$/GATA6$^{+}$ (G6+) and NANOG$^{+}$/GATA6$^{+}$ (N+ G6+) populations at E3.25 ($n$=16 embryos), E3.5 ($n$=9) and E3.75 ($n$=11). (E) Expression in two representative E4.5 embryos ($n$=6) showing ERK phosphorylation in some PrE cells labelled by GATA6 (red arrowheads), in some Epi cells (white arrowheads) and in some outside/TE cells (yellow arrowheads). Scale bars: 10 µm.

Development (2019) 146, dev177139. doi:10.1242/dev.177139

consistent with required pERK activity for TE proliferation (Nichols et al., 2009). Then, we determined the identity of pERK-labelled ICM cells by examining NANOG and GATA6 levels at each developmental stage (Fig. 1B,D). Cell counts indicated that very few cells were labelled between E3.0 and E3.25 (Fig. 1C), around two to three per embryo, with a relatively weak staining that was present in uncommitted cells that are doubly positive for NANOG and GATA6 (Bessonnard et al., 2014, 2017; Plusa et al., 2008; Saiz et al., 2016) (Fig. 1D). Subsequently, the number of cells with a strong pERK staining gradually increased (Fig. 1C) and they progressively corresponded to PrE cells solely labelled by GATA6 (Fig. 1D). Thus, ERK phosphorylation essentially occurs in PrE-specified cells as well as in a subset of uncommitted cells, implying induction of their specification into PrE cells. However, not all PrE cells were labelled by pERK whereas all PrE cells require FGF/ERK activity for their specification (Chazaud et al., 2006; Kang et al., 2017; Molotkov et al., 2017; Nichols et al., 2009; Yamanaka et al., 2010). This low frequency of labelled cells may reflect a transient nature of pERK labelling.

### pERK is present during postimplantation development and in cultured embryonic stem cells

After cell specification into Epi and PrE, little is known about MAPK activity in the three cell lineages during their further differentiation. From E4.0, several FGF ligand genes are expressed in the Epi (*Fgf4*, *Fgf5*, *Fgf8*, *Fgf15*, *Fgf18*) and in the PrE (*Fgf3*, *Fgf17*), and can be transduced by *Fgfr1*, *Fgfr2*, *Fgfr3* or *Fgfr4* (Ohnishi et al., 2014). Moreover, PDGF signalling has been shown to be important for PrE cell survival (Artus et al., 2013) and could act through the MAPK pathway. Accordingly, pERK was detected in PrE cells at E4.5 (Fig. 1E) and their derivatives at E6.5 (Fig. S3A). Consistent with a previous report (Corson et al., 2003), strong pERK signals were detected in the extra-embryonic ectoderm of E6.5 embryos (Fig. S3A).

In FGF/ERK-impaired embryos, NANOG levels are maintained in the E4.5 Epi whereas they decay in wild-type (WT) embryos (Kang et al., 2013; Molotkov et al., 2017; Nichols et al., 2009). This suggests that FGF4 enables Epi maturation by downregulating NANOG levels. Accordingly, we could observe ERK phosphorylation in some Epi cells at E4.5 (Fig. 1E), most likely through the transduction of FGFR1, the only FGF receptor expressed in this tissue at this stage (Ohnishi et al., 2014). Similarly, mouse embryonic stem (ES) cells, which are closely related to the E4.5 Epi (Boroviak et al., 2014), express high levels of *Fgf4*, and the FGF pathway is necessary for their exit of pluripotency and differentiation (Hamilton and Brickman, 2014; Kalkan et al., 2017; Kunath et al., 2007; Molotkov et al., 2017; Schröter et al., 2015; Stavridis et al., 2010). Heterogeneous labelling was observed among the cells (Fig. S3B) (Deathridge et al., 2019; Hamilton and Brickman, 2014), possibly due to heterogeneous levels of NANOG between cells (Chambers et al., 2007) that are controlling *Fgf4* secretion, and also owing to possible transient ERK phosphorylation. In the presence of the MEK inhibitor, pERK staining was strongly diminished in ES cells (Fig. S3B).

We thus report that the ERK pathway is active in the three cell lineages derived from Epi, PrE and TE.

### Analysis of *Fgf4*, *Klf5*, *Nanog* and *Gata6* mutant embryos reveals upstream regulation of FGF/pERK

*Fgf4* is specifically expressed in Epi cells (Frankenberg et al., 2011; Guo et al., 2010; Kurimoto et al., 2006; Ohnishi et al., 2014) and acts as a paracrine factor to differentiate neighbouring cells (Frankenberg et al., 2011). *Fgf4* targeted inactivation leads to an absence of PrE cells and pan-expression of Epi markers in the ICM (Kang et al., 2013; Krawchuk et al., 2013). ERK phosphorylation was not detected in *Fgf4* knockout embryos (Fig. 2A) demonstrating that FGF4 is the sole secreted signal activating the ERK pathway at this stage of development.

Our previous results showed that *Klf5* is essential for blastocyst development (Ema et al., 2008). Indeed, through direct binding to *Fgf4* regulatory elements, KLF5 prevents precocious expression of *Fgf4* at E3.0-E3.25 to initiate cell differentiation at the right time and to ensure a proper balance between Epi and PrE cells (Azami et al., 2017). Consistent with our previous study, $Klf5^{-/-}$ embryos at E3.25 had a stronger pERK signal and in more cells compared with that of WT embryos (Fig. 2B).

We have previously shown (Frankenberg et al., 2011) that *Fgf4* transcription in Epi cells requires the presence of NANOG (Fig. 2E). As expected, in *Nanog* mutant embryos, the lack of FGF4 led to an absence of pERK (Fig. 2C).

Removing one or two alleles of *Gata6* increased the number of *Fgf4*-expressing cells (Fig. 2E) as more cells produce NANOG (Bessonnard et al., 2014). As a consequence, pERK staining could be observed in a higher number of ICM cells in $Gata6^{-/-}$ embryos (Fig. 2D), owing either to transcriptional activation of *Fgf4* by NANOG, or to a lack of GATA6 repression (Fig. 2E). It is interesting to note that ICM cells in $Gata6^{-/-}$ embryos have an Epi identity and are nevertheless able to transduce FGF signalling through FGFR1, which is expressed in these cells (Fig. 2E). This ERK activity is reminiscent of what is found in E4.5 WT Epi cells or in ES cells.

### DUSP4 but not ETV5 is positively regulated by pERK

ETVs and DUSP4 are considered as direct targets of the MAPK/ERK pathway (Neben et al., 2017; Patel and Shvartsman, 2018) and are present in the blastocyst (Guo et al., 2010; Kang et al., 2017; Kurimoto et al., 2006). We carried out single-cell RNA analyses, and we subdivided the samples between *Fgf4*-expressing ($Fgf4^{+}$) and *Fgf4*-non expressing ($Fgf4^{-}$) populations as *Fgf4* was identified as the Epi marker with the earliest binary expression (Guo et al., 2010; Ohnishi et al., 2014). Transcripts of *Dusp4* were barely detected at the 16-cell stage and later were preferentially expressed in $Fgf4^{-}$ cells identified as PrE cells (Fig. 3A). By contrast, *Etv5* expression was enriched in $Fgf4^{+}$ Epi cells as early as E3.25 (Fig. 3A; see Fig. S4D for RNA-seq data analysis, data taken from Posfai et al., 2017). *Etv4* expression started from E3.5, thus after the beginning of Epi/PrE specification (Fig. 3A, Fig. S4D). At E3.75, when the NANOG/GATA6 mutually exclusive pattern is established, *Etv4* was enriched in $Fgf4^{-}$ PrE cells whereas *Etv5* was enriched in $Fgf4^{+}$ Epi cells (Fig. 3A).

At E3.25, the protein DUSP4 was observed in some outside cells corresponding to TE (Fig. S4A) as reported for its RNA localisation (Posfai et al., 2017), consistent with an active FGF pathway to promote TE growth (Nichols et al., 2009). Later, DUSP4 localised to PrE cells (Fig. 3B,C) but could also be found in undifferentiated cells, labelled by both GATA6 and NANOG, especially at the beginning of blastocyst formation (Fig. 3C). DUSP4 could not be detected in Epi cells (Fig. 3C). Double labelling with pERK and DUSP4 antibodies showed a high correlation of expression (Fig. 3B). However, some pERK-only marked cells could be observed, probably reflecting an early activation of the pathway just preceding a visible DUSP4 translation. As well, DUSP4-only labelled cells were found, illustrating a plausible transient nature of ERK activation. As expected, the number of DUSP4-labelled cells was enhanced by FGF2 treatment and no signal could be detected upon MEK inhibitor administration (Fig. S4B).

Development (2019) 146, dev177139. doi:10.1242/dev.177139

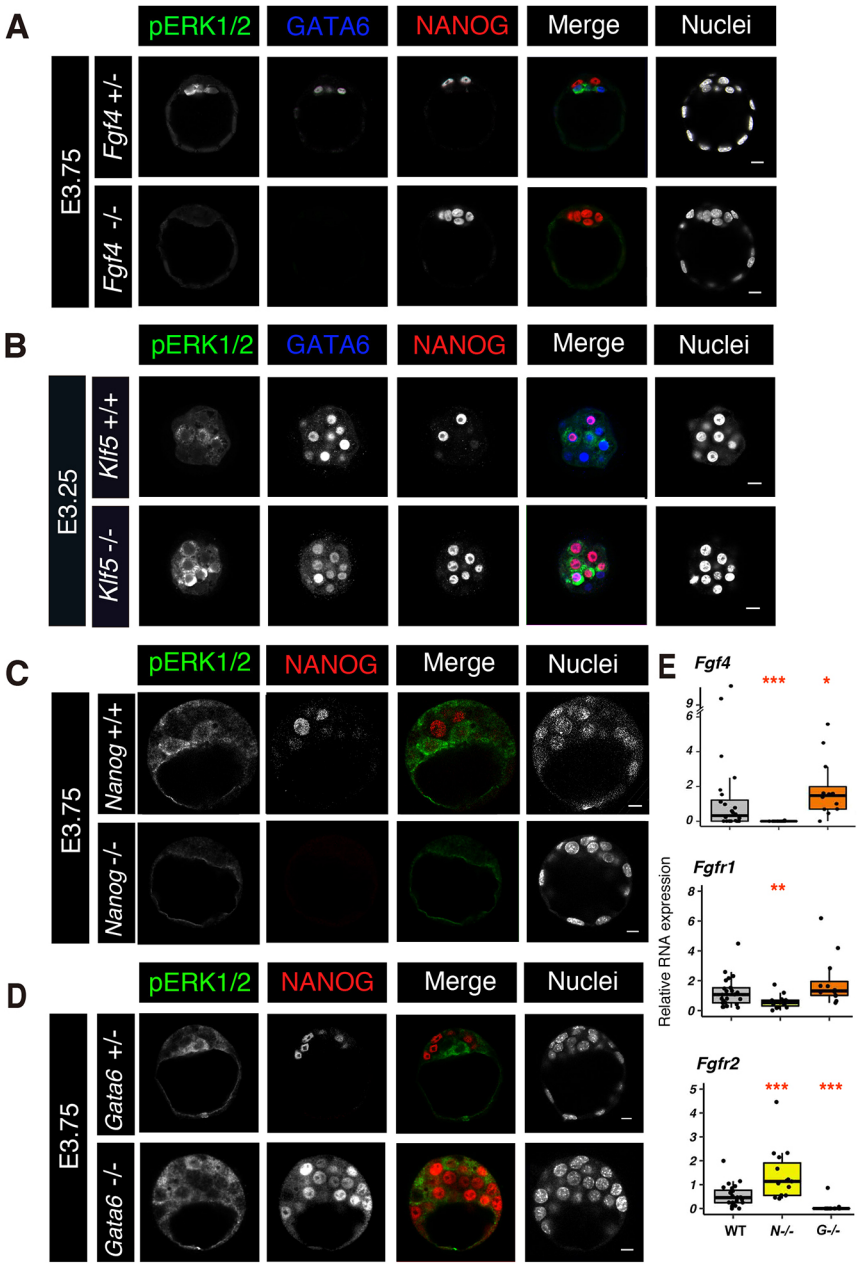


**Fig. 2. ERK phosphorylation in mutant embryos during preimplantation.** (A) pERK, NANOG and GATA6 staining in *Fgf4* mutants (WT, *n*=12; *Fgf4*$^{-/-}$ *n*=5). (B) pERK, NANOG and GATA6 detection in *Klf5* mutants (WT, *n*=14; *Klf5*$^{-/-}$ *n*=5). (C) pERK and NANOG labelling in *Nanog* mutants (WT, *n*=5; *Nanog*$^{-/-}$ *n*=5). (D) pERK and NANOG detection in *Gata6* mutants (Ctrl, *n*=7; *Gata6*$^{-/-}$, *n*=5). (E) Single-cell RNA expression of *Fgf4*, *Fgfr1* and *Fgfr2* in individual ICM cells isolated from *Nanog*$^{-/-}$ (*N*$^{-/-}$; *n*=15 cells), *Gata6*$^{-/-}$ (*G*$^{-/-}$; *n*=13 cells) and WT (*n*=24 cells) embryos at E3.25. Red asterisks indicate significant differences of expression between mutant and WT samples (Wilcoxon tests: **P*<0.05, ***P*<0.01, ****P*<0.001). Scale bars: 10 µm.

In *Nanog* mutants, DUSP4 was poorly detected in the ICM (Fig. 3D), in accordance with the absence of *Fgf4* in these embryos (Fig. 2E; Frankenberg et al., 2011). By contrast, DUSP4 labelling was observed in some cells in *Gata6*$^{-/-}$ embryos (Fig. 3D). This result shows that DUSP4 does not need GATA6 presence to be expressed but relies essentially on pERK signalling activity. Alternatively, this expression in the Epi of *Gata6*$^{-/-}$ embryos could correspond to cells exiting pluripotency, as ES cells in transition from naïve pluripotency express DUSP4 (Kalkan et al., 2017). Indeed, we have previously shown that Epi specification is more precocious in these mutants (Bessonnard et al., 2014), and this most likely leads also to an earlier Epi transition to a mature state.

ETV5 is an ETS-related transcription factor involved in the transduction of the MAPK pathway (Herriges et al., 2015; Sharrocks, 2001) and is expressed in the blastocyst ICM (Guo et al., 2010; Kang et al., 2017). By immunofluorescence, we showed that from E3.5 ETV5 is preferentially observed in Epi cells as it colocalises with NANOG mainly (Fig. 4A, Fig. S4C), confirming RNA expression data (Fig. 3A); however, some PrE cells also expressed the protein (Fig. S4C). Surprisingly, ETV5 labelling was lost upon FGF2 administration and was present in more cells upon administration of MEK and FGFR inhibitors (Fig. 4A). Thus, ETV5 does not behave like a MAPK signalling reporter but instead acts as an Epi marker. Strikingly, ETV5 levels were drastically downregulated in *Nanog*$^{-/-}$ embryos and the protein was present throughout the ICM of *Gata6*$^{-/-}$ embryos (Fig. 4B). Therefore, our data clearly indicate that ETV5 is not positively regulated by RTK signals but by the presence of NANOG during blastocyst formation.

## DISCUSSION

FGF signalling, through FGFR and ERK, controls PrE differentiation in the ICM of the mouse blastocyst (Brewer et al., 2016; Chazaud et al., 2006; Feldman et al., 1995; Kang et al., 2013, 2017; Krawchuk et al., 2013; Molotkov et al., 2017; Nichols et al.,

Development (2019) 146, dev177139. doi:10.1242/dev.177139

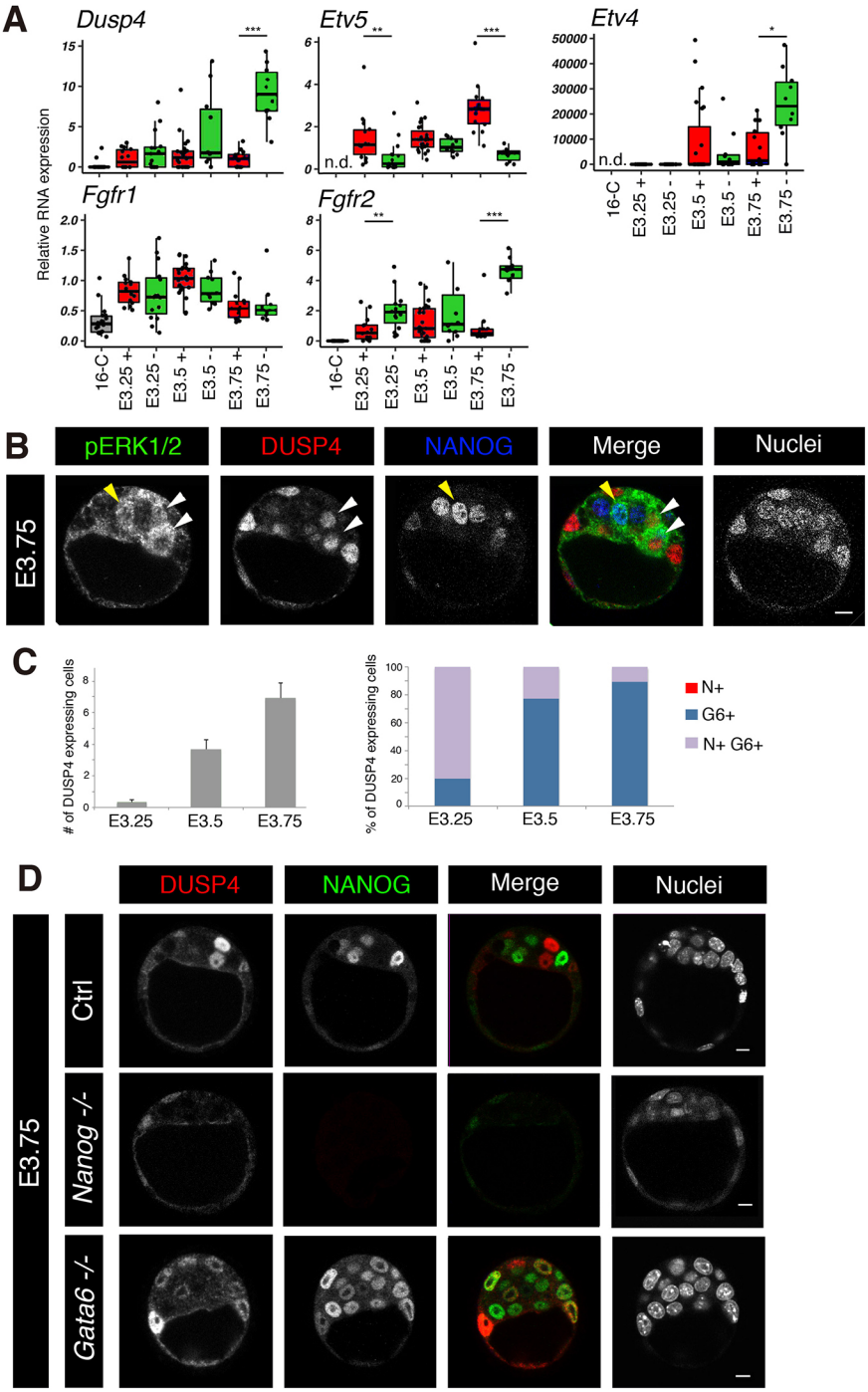


**Fig. 3. Expression of FGF pathway-related genes.** (A) Single-cell RNA expression of *Dusp4*, *Etv5*, *Etv4*, *Fgfr1* and *Fgfr2* in 16-cell stage embryos ($n$=18 cells) and in ICMs at E3.25 ($n$=29 cells), E3.5 ($n$=33 cells) and E3.75 ($n$=24 cells). At the later stages, ICM populations were subdivided into two groups defined by the presence (+, red boxes) or absence (–, green boxes) of *Fgf4* expression in the cell. This enables discrimination between Epi (+) and PrE (–) cells. Experiments at the 16-cell stage were not carried out for *Etv4* and *Etv5* (n.d., not determined). Asterisks indicate significant differences of expression between *Fgf4*$^+$ and *Fgf4*– cells (Wilcoxon tests: *$P$<0.05, **$P$<0.01, ***$P$<0.001). (B) Detection of pERK and DUSP4 ($n$=21) with NANOG at E3.75. White arrowheads point to cells that express both pERK and DUSP4. Yellow arrowheads point to a cell expressing pERK but not DUSP4, most likely a precursor cell that still expresses NANOG. (C) Number of DUSP4-expressing cells per ICM at E3.25 ($n$=15 embryos), E3.5 ($n$=18) and E3.75 ($n$=11). Data are represented as mean±s.e.m. The right panel indicates the distribution of ICM DUSP4-labelled cells between NANOG$^+$/GATA6$^-$ (N+), NANOG$^-$/GATA6$^+$ (G6+) and NANOG$^+$/GATA6$^+$ (N+ G6+) populations. (D) Detection of DUSP4 and NANOG in *Nanog*$^{-/-}$ (Ctrl, $n$=12; *Nanog*$^{-/-}$ $n$=12/15 with no DUSP4$^+$ cells and 3/15 with one to three DUSP4$^+$ cells in the ICM) and *Gata6*$^{-/-}$ (Ctrl, $n$=6; *Gata6*$^{-/-}$, $n$=9/12 with some ICM DUSP4$^+$ cells) in E3.5-E3.75 embryos. Scale bars: 10 µm.

2009; Saiz et al., 2016; Yamanaka et al., 2010). However, the spatiotemporal expression of active, phosphorylated ERK has never been reported during mouse preimplantation development. We show here that ERK phosphorylation begins at the onset of Epi/PrE differentiation, around E3.25, when *Fgf4* transcripts start to be elevated in some ICM cells (Ohnishi et al., 2014). Thus, as soon as *Fgf4* is expressed at sufficient levels, ERK phosphorylation can be observed. This phosphorylation is present essentially in uncommitted cells, doubly labelled by NANOG and GATA6, and in PrE cells solely marked by GATA6. This is consistent with the known pERK activity of converting uncommitted cells into PrE (Bessonnard et al., 2017; Saiz et al., 2016) and our data show here that ERK phosphorylation can be seen in PrE cells up to at least E4.5. At this stage, pERK is also observed in some Epi cells, when they are differentiating further through a formative phase (Smith, 2017). Interestingly, NANOG is maintained in the ICM of *Fgf4* and in *Fgfr1/Fgfr2* mutants at E4.5 (Kang et al., 2013; Molotkov et al., 2017), indicating that Epi maturation requires FGF signalling, which is consistent with the observed ERK phosphorylation.

DUSP phosphatases have been shown to be transcriptional ERK targets in several models and inhibit the FGF pathway in a negative-feedback loop through dephosphorylation of ERK (Amit et al., 2007; Brewer et al., 2016; Chu et al., 1996; Eblaghie et al., 2003; Ekerot et al., 2008; Lemmon and Schlessinger, 2010; Niwa et al., 2007). We show that DUSP4 accumulation tightly follows ERK phosphorylation, and depends on it. In WT embryos, DUSP4

Development (2019) 146, dev177139. doi:10.1242/dev.177139

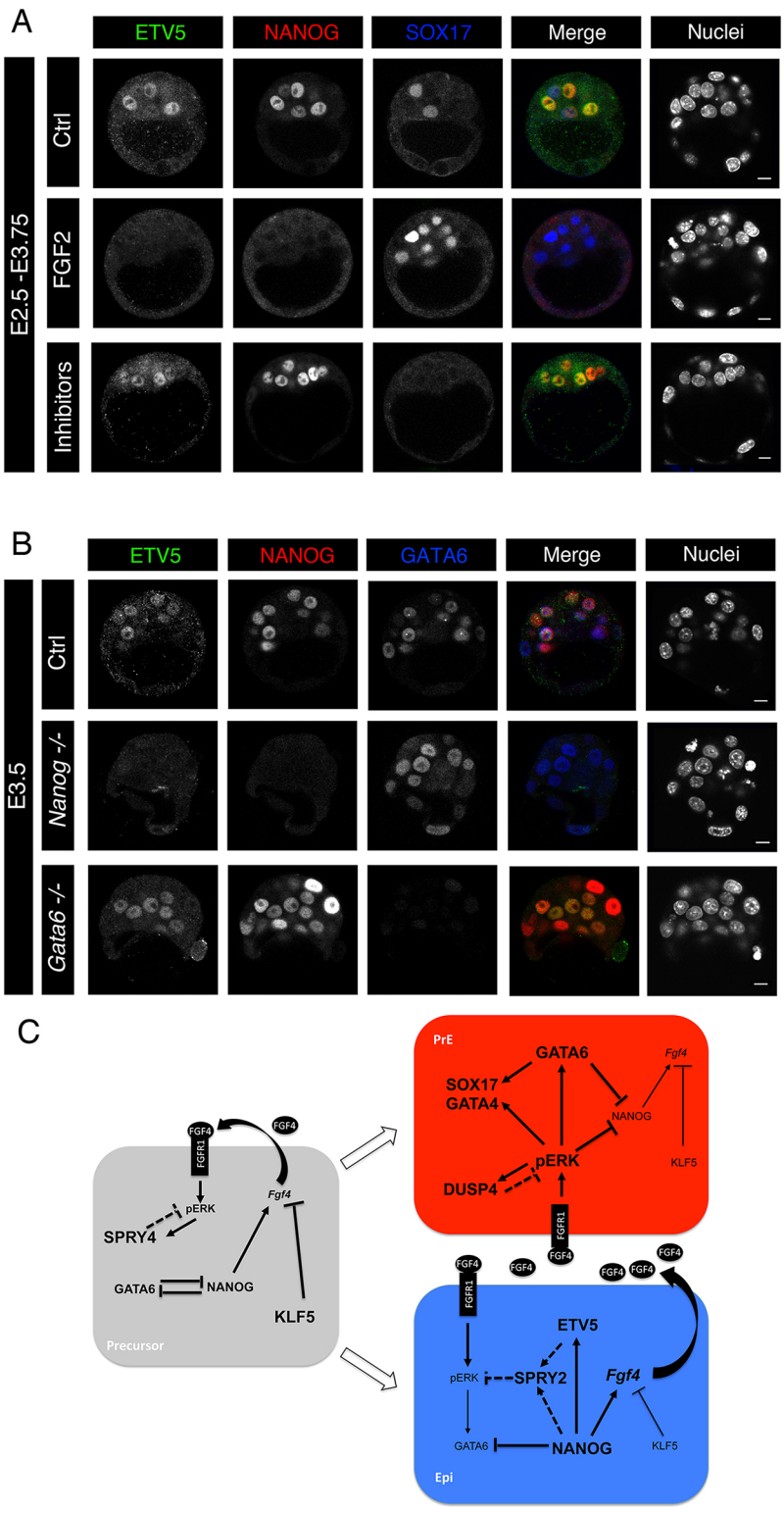


**Fig. 4. Expression of ETV5.** (A) Immunostaining of ETV5, together with NANOG and SOX17, in embryos cultured with either FGF2 ($n$=6), MEK+FGFR inhibitors ($n$=17) or untreated embryos (Ctrl, $n$=16) from E2.5 to E3.75. (B) ETV5 expression in *Nanog*$^{-/-}$ (Ctrl, $n$=5; *Nanog*$^{-/-}$, $n$=4/6 with no ETV5$^{+}$ and 2/6 with one ETV5$^{+}$ cell) and *Gata6*$^{-/-}$ (Ctrl, $n$=6; *Gata6*$^{-/-}$$n$=6) embryos. Scale bars: 10 µm. (C) Working model. In precursor cells (16-cell/E3.25 stage) that co-express NANOG and GATA6, KLF5 and possibly SPRY4 inhibit the FGF pathway. KLF5 expression decreases during blastocyst growth. Precursor cells can differentiate into either Epi or PrE between E3.25 and E3.75 in an asynchronous manner. In Epi cells, NANOG induces the expression of both *Fgf4* and *Etv5*. Upon ETV5 induction, or possibly NANOG induction, SPRY2 inhibits the ERK pathway, protecting the cell from autocrine as well as paracrine FGF4. In PrE (or future PrE) cells, pERK is activated by FGF4 secreted from neighbouring Epi cells, leading to maintenance of GATA6 levels and downregulation of NANOG levels. Together with pERK, GATA6 induces downstream PrE genes such as *Sox17* and *Gata4*. DUSP4 is activated by pERK independently of *Gata6*. It possibly resensitises the FGF pathway by de-phosphorylating ERK. Thick connections represent activated interactions, thin arrows show tamed or extinct interactions and dashed lines are suggested activities.

could be considered as a PrE marker; however, its expression in *Gata6*$^{-/-}$ embryos, which do not contain PrE cells, indicates that this protein is linked to pERK activity rather than PrE identity and is thus a reliable ERK activity reporter. Co-labelling experiments of pERK with DUSP4 suggest transient activation of ERK whereas DUSP4 presence is more robust. Transient or sustained ERK activities have been observed downstream of RTK signalling to control different cellular responses. These differences in the output, despite sharing signalling intermediates, can be explained in part by differences in feedback mechanisms (Lemmon and Schlessinger, 2010). The rather transient nature of the pERK labelling observed during preimplantation suggests the presence of negative-feedback loops that could be mediated through DUSP4.

ETS-related molecules such as ETV4 and 5, are transcriptionally activated by the FGF pathway in several different developmental processes and tissues (Aulehla et al., 2008; Liu et al., 2003; Raible

Development (2019) 146, dev177139. doi:10.1242/dev.177139

and Brand, 2001; Roehl and Nüsslein-Volhard, 2001). ETS factors are often involved in positive- or negative-feedback loops of ERK signalling (Herriges et al., 2015; Reginensi et al., 2011), being either activators or repressors of transcription and potentially regulating negative effectors of the pathway, such as SPROUTYs (SPRYs) (Hacohen et al., 1998; Herriges et al., 2015; Neben et al., 2017; Sharrocks, 2001). *Etv4*, *Etv5* and *Spry4* have been reported to be expressed in both Epi and PrE cells during blastocyst formation, whereas *Spry2* is preferentially expressed in the Epi (Boroviak et al., 2015; Kang et al., 2017; Morgani et al., 2018). Moreover, *Etv4* and *Spry4* respond to FGF/ERK signalling (Kang et al., 2017; Morgani et al., 2018). It was then proposed that these ETVs and SPRYs would suppress or dampen ERK activity through a FGF negative-feedback loop, to desensitise Epi cells from their own FGF4 secretion (Kang et al., 2017). However, we found that pERK is almost undetectable in blastocyst Epi cells, implying either that *Etv4* and *Spry4* are only transcribed in precursor cells with a high RNA stability, or that these genes can respond to very low levels of pERK, or that their expression depends also on other factors. Data extraction from single-cell RNA-seq analyses (Posfai et al., 2017) show that only *Spry4*, but not *Etv4*, is expressed in precursor cells at the 16-cell stage (Fig. S4D). Thus, SPRY4, under FGF stimulation, could tame the FGF/ERK pathway at least in the precursor cells.

*Spry2* is particularly interesting because its transcripts are differentially enriched between Epi and PrE cells (Boroviak et al., 2015; Kang et al., 2017). Indeed, FGF signalling must not be blocked in PrE cells. SPRY2 protein is present in ES cells (Christoforou et al., 2016), and, similar to its transcripts (Fig. S4), the levels of this protein increase between the morula and blastocyst stages (Gao et al., 2017). In *Fgfr* mutants, *Spry2* expression is maintained at E3.5 and then downregulated by the late blastocyst stage (Kang et al., 2017), indicating that its initial expression is independent of FGF signalling. ETS-binding sites have been characterised in the human *SPRY2* promoter (Ding et al., 2003), and they are conserved in the mouse. Thus, SPRY2 is a good candidate downstream of ETVs to block FGF signalling in the Epi, as early as the 16-cell/E3.25 stage (Fig. S4D); however, we cannot exclude the possibility that other negative factors, such as SPREDs or RSKs (Mühl et al., 2015; Neben et al., 2017; Nett et al., 2018), might be at play. We show here that *Etv5* transcripts, like those of *Spry2*, and protein are enriched in EPI cells. Surprisingly, ETV5 levels are not positively regulated by the FGF/ERK pathway but depend on the presence of NANOG, likely through direct activation as NANOG binds to the *Etv5* locus in ES cells (Boyer et al., 2005; Loh et al., 2006; Murakami et al., 2016). Thus, this reveals a novel potential mechanism by which NANOG activates the expression of FGF4 and ETV5 at the same time, on one hand to induce paracrine PrE cell differentiation, and on the other hand to protect Epi cells against autocrine/paracrine FGF4 activity. This mechanism of direct activation of ETV5 by NANOG would seem to be a more efficient way to protect the identity of Epi cells compared with activation of ETV5 through a negative-feedback loop found in other systems (Herriges et al., 2015). Indeed, ETV5 is already present when Epi cells are subjected to autocrine/paracrine FGF4 activity.

How ERK activity is controlled during Epi/PrE specification has remained unclear. With these novel data we propose (Fig. 4C) that in precursor cells of the early ICM, expressing both NANOG and GATA6, pERK activity remains very low or absent due to (1) KLF5 presence that limits the number of *Fgf4* transcripts (Azami et al., 2017) and (2) possible inhibition of the FGF pathway by a negative-feedback mechanism through SPRY4 (Kang et al., 2017; Morgani et al., 2018). Then at the beginning of Epi specification, NANOG levels become predominant over GATA6 levels, enabling the transcription of both *Fgf4* and *Etv5*. FGF4 is secreted and binds to FGFR1, which is equally expressed among ICM cells. In Epi cells, ETV5 is likely to protect the cells from the surrounding FGF4 by activating negative regulators of the FGF pathway, such as SPRY2, to attenuate or block the pERK signals. In PrE cells, NANOG is not expressed and therefore ETV5 is absent. This enables efficient FGF/ERK pathway activity, illustrated by DUSP4 expression, to differentiate the cells into PrE by maintaining a high expression of GATA6 and inducing downstream PrE factors such as SOX17 and GATA4.

In conclusion, our results show that NANOG is key to binary cell differentiation by activating within the same cell the differentiation paracrine cues and a protective cell-autonomous mechanism.

## MATERIALS AND METHODS

### Embryo collection and culture

Preimplantation embryos obtained from natural matings [CD1 (ICR) background] were collected from oviducts or uteri by flushing with M2 medium (Sigma-Aldrich). Embryos were cultured in the presence of MEK inhibitor (PD0325901; 0.5 µM) (Selleck), FGFR inhibitor (PD173074; 100 nM) (Selleck), FGF2 (Cell Guidance Systems) or FGF4 (1 µg/ml) (R&D)+heparin(1 µg/ml) (Sigma-Aldrich) in KSOM+AA medium (Millipore) in 4-well plates at 37°C, 5% $CO_2$. All experiments were replicated at least three times.

### Mutant mice

*Fgf4*$^{tm1.2Mrt}$ (Sun et al., 2002), obtained from MMRRC at UC Davis, were crossed with Ayu1-Cre mice, which express Cre recombinase from the zygote to generate the deletion of *Fgf4* allele. *Fgf4*$^{+/-}$ mice were then intercrossed to obtain *Fgf4* mutant embryos. *Nanog* and *Gata6* mutant embryos were obtained as previously described (Bessonnard et al., 2014; Frankenberg et al., 2011; Mitsui et al., 2003; Sodhi et al., 2006) through natural matings. *Klf5* knockout embryos were generated as previously described (Azami et al., 2017). All mice were maintained on the CD1 (ICR) background. Embryo genotyping was performed after confocal imaging, as described previously (Azami et al., 2017; Bessonnard et al., 2014; Frankenberg et al., 2011). Experiments were performed in accordance with French/EU and Japanese guidelines for the care and use of laboratory animals. Experimental procedures were approved by the Animal Care and Use Committee of Shiga University of Medical Science and methods were carried out in accordance with the approved guidelines (approval number: 2016-11-8, 2018-10-1). All animal work was conducted according to French and European directives for the use and care of animals for research purposes and was approved by the local ethics committee, C2E2A (Comité d'Ethique pour l'Expérimentation Animale en Auvergne).

### Whole-mount immunostaining

Immunostaining of embryos was performed as described previously (Azami et al., 2017). Briefly, embryos were fixed in 4% paraformaldehyde (PFA) in 1×PBS for 15-30 min at room temperature (RT). Permeabilisation was performed in 0.5% Triton X-100 in PBS for 15 min and embryos were incubated in blocking solution [1% donkey serum, 0.1% bovine serum albumin (BSA) and 0.01% Tween 20 in PBS] for 1 h at RT. Then, embryos were treated with primary antibodies in blocking solution overnight at 4°C. After washing with 0.1% Tween 20 in PBS three times, embryos were treated with secondary antibodies (made in donkey, Jackson Laboratories, 1/300) in blocking solution for 1 h at RT. Nuclei were stained with Hoechst 33342 (Thermo Fisher) or DAPI and cell membranes with phalloidin (1/1000, Jackson ImmunoResearch). To visualise DUSP4, a tyramide signal amplification (TSA) reaction was carried out according to manufacturer's instructions (Thermo Fisher or Perkin Elmer). Double immunostaining for pERK and DUSP4, e.g. with antibodies from the same host, was performed by a sequential immunostaining of pERK and then DUSP4. Briefly, after the TSA reaction with the first rabbit antibody, the horseradish peroxidase (HRP) was inactivated by a treatment of 5 min 3% $H_2O_2$ in PBS. Then, the

Development (2019) 146, dev177139. doi:10.1242/dev.177139

second rabbit primary antibody staining was carried out as usual (as control, the second primary antibody was not added to ascertain the inactivation of the first HRP). Primary antibodies are listed in Table S1.

### Phosphorylated ERK staining

Visualisation of phosphorylated ERK (pERK) was performed following two protocols.

#### pERK staining with 8% PFA

Embryos collected from uterus or oviducts were precultured in KSOM+AA medium at 37°C, 5% $CO_2$. They were fixed in 8% PFA together with phosphatases inhibitors: NaF (25 mM, Sigma-Aldrich), sodium orthovanadate (2 mM, NEB) and β-glycerophosphate (50 mM, Santa Cruz Biotechnology) for 10 min at RT. They were permeabilised 5 min in 0.5% Triton X-100/PBS and non-specific sites were blocked with 10% fetal bovine serum/0.1% Triton X-100/PBS for 30 min. Primary antibodies were added to the blocking solution overnight at 4°C. After three washes, secondary antibodies coupled to peroxidase were added and TSA reaction was carried out according to manufacturer's instructions (Thermo Fisher or Perkin Elmer).

#### pERK staining with ProK

Embryos collected from uterus or oviducts were precultured in KSOM+AA medium at 37°C, 5% $CO_2$ and fixed in 4% PFA with PhosSTOP (Roche) for 20 min on ice. Embryos were permeabilised and activated with 10 ng/ml proteinase K (ProK) (Roche) in 0.1% Tween 20/PBS at RT for 3-5 min, depending on the developmental stage. The ProK reaction was stopped in 2 mg/ml glycine-PBS for 2 min at RT and embryos were washed in 0.1% Tween 20/PBS. Blocking was performed in 0.5% donkey serum/0.5% casein/0.5% BSA in PBS for 30 min at RT. Then, embryos were treated with the primary antibody in blocking solution overnight at 4°C. After washing with 0.1% Tween 20 in PBS three times, embryos were treated with HRP-conjugated secondary antibody in blocking solution for 1 h at RT. TSA (Thermo Fisher) was used to detect pERK signal.

### Confocal microscope and image analyses

Leica TCS SP8, SP5 or SPE confocal microscopes were used to acquire the fluorescent images of immunostained embryos as described previously (Azami et al., 2017; Gasnier et al., 2013). Look up table (LUT) visualisation of fluorescence intensity was processed using Fiji. The 'thermal' range of LUT indicates high levels of expression in red and low levels in blue. Unless otherwise indicated, images are displayed as single *z*-sections representative of the embryo. Cell counts were performed as previously described (Bessonnard et al., 2014).

### Single-cell RT-qPCR analyses

Isolated ICM cells (after immunosurgery; Nagy, 2003) and morulae (16°C) were incubated for 10 min in 1×TrypLE Express Enzyme (Gibco) at 37°C and cells were isolated by repeated mouth pipetting using pulled capillaries of serially smaller diameter openings. Each single cell was collected in 5 µl of 2× Reaction Mix (Invitrogen, CellsDirect One-Step qRT-PCR Kit) and stored at −80°C or processed immediately. Genotyping of embryos was carried out using TE cells from immunosurgery with whole genome amplification (WGA) using the REPLI-g kit (Qiagen) followed by PCR genotyping as above.

cDNA from the desired genotypes was preamplified with 18 cycles. Quality and genotype checks were performed by qPCR for each cell with housekeeping gene primers (*Rps17* and *Rpl30*) and primers detecting the mutations. The analysed cells originate from at least three different embryos in each category.

Single-cell qPCR on a Fluidigm Biomark system (GENTYANE facility) was carried out on 48.48 or 96.96 Dynamic Arrays, according to the manufacturer's instructions. Cells with absent or low Ct values for the housekeeping genes *Rps17* and *Rpl30* were removed from the analysis (5%). Ct values were normalised with the mean of housekeeping genes *Rps17* and *Rpl30* using the 2-ΔCt method. In box plots, values are relative to the mean of all WT E3.25 cells to be able to compare between genotypes and stages. Cells were considered in $Fgf4^{-}$ subpopulations when CT values were above 35 and all other cells were placed in $Fgf4^{+}$ subpopulations. Primers used for this study are listed in Table S2.

For the box plots, the edges of the box represent 25th and 75th quartiles. The median is represented by the central line. The whiskers extend to 1.5 times the interquartile range (25th to 75th percentile). Cells are plotted individually in single-cell experiments.

### Statistical analyses

Statistical tests were performed using Graphpad software. Statistical significance was assessed using the Wilcoxon-Mann–Whitney test (non-parametric) on expression levels. Unless otherwise indicated, the phenotypes are fully penetrant.

#### Acknowledgements

Images were acquired and treated at the CLIC imaging facility (Clermont-Fd). C.C. thanks C. Pléver for genotyping the mice.

#### Competing interests

The authors declare no competing or financial interests.

#### Author contributions

Conceptualization: T.A., M.E., C.C.; Methodology: T.A., C.B., N.A., C.C.; Software: P.P.; Validation: T.A., C.B., N.A., L.V.E., M.E., C.C.; Formal analysis: T.A., C.B. and P.P.; Investigation: T.A., C.B., N.A., L.V.E., C.C.; Resources: N.A., L.V.E.; Writing - original draft: T.A., C.B., C.C.; Writing - review & editing: T.A., M.E., C.C.; Visualization: C.B., N.A., P.P., C.C.; Supervision: M.E., C.C.; Project administration: M.E., C.C.; Funding acquisition: M.E., C.C.

#### Funding

C.C. was supported by the Agence Nationale de la Recherche ('PrEpiSpec') and the Fondation pour la Recherche Médicale. T.A. was supported by Japan Society for the Promotion of Science Grants-in-Aid for Young Scientists (17K14976).

#### Supplementary information

Supplementary information available online at
http://dev.biologists.org/lookup/doi/10.1242/dev.177139.supplemental

#### References

**Amit, I., Citri, A., Shay, T., Lu, Y., Katz, M., Zhang, F., Tarcic, G., Siwak, D., Lahad, J., Jacob-Hirsch, J. et al.** (2007). A module of negative feedback regulators defines growth factor signaling. *Nat. Genet.* **39**, 503-512. doi:10.1038/ng1987

**Artus, J., Kang, M., Cohen-Tannoudji, M. and Hadjantonakis, A.-K.** (2013). PDGF signaling is required for primitive endoderm cell survival in the inner cell mass of the mouse blastocyst. *Stem Cells* **31**, 1932-1941. doi:10.1002/stem.1442

**Aulehla, A., Wiegraebe, W., Baubet, V., Wahl, M. B., Deng, C., Taketo, M., Lewandoski, M. and Pourquié, O.** (2008). A β-catenin gradient links the clock and wavefront systems in mouse embryo segmentation. *Nat. Cell Biol.* **10**, 186-193. doi:10.1038/ncb1679

**Azami, T., Waku, T., Matsumoto, K., Jeon, H., Muratani, M., Kawashima, A., Yanagisawa, J., Manabe, I., Nagai, R., Kunath, T. et al.** (2017). Klf5 maintains the balance of primitive endoderm to epiblast specification during mouse embryonic development by suppression of Fgf4. *Dev. Camb. Engl.* **25**, dev.150755. doi:10.1242/dev.150755

**Bessonnard, S., De Mot, L., Gonze, D., Barriol, M., Dennis, C., Goldbeter, A., Dupont, G. and Chazaud, C.** (2014). Gata6, Nanog and Erk signaling control cell fate in the inner cell mass through a tristable regulatory network. *Dev. Camb. Engl.* **141**, 3637-3648. doi:10.1242/dev.109678

**Bessonnard, S., Coqueran, S., Vandormael-Pournin, S., Dufour, A., Artus, J. and Cohen-Tannoudji, M.** (2017). ICM conversion to epiblast by FGF/ERK inhibition is limited in time and requires transcription and protein degradation. *Sci. Rep.* **7**, 12285. doi:10.1038/s41598-017-12120-0

**Boroviak, T., Loos, R., Bertone, P., Smith, A. and Nichols, J.** (2014). The ability of inner cell mass cells to self-renew as embryonic stem cells is acquired upon epiblast specification. *Nat. Cell Biol.* **16**, 516-528. doi:10.1038/ncb2965

**Boroviak, T., Loos, R., Lombard, P., Okahara, J., Behr, R., Sasaki, E., Nichols, J., Smith, A. and Bertone, P.** (2015). Lineage-specific profiling delineates the emergence and progression of naive pluripotency in mammalian embryogenesis. *Dev. Cell* **35**, 366-382. doi:10.1016/j.devcel.2015.10.011

**Boyer, L. A., Lee, T. I., Cole, M. F., Johnstone, S. E., Levine, S. S., Zucker, J. P., Guenther, M. G., Kumar, R. M., Murray, H. L., Jenner, R. G. et al.** (2005). Core transcriptional regulatory circuitry in human embryonic stem cells. *Cell* **122**, 947-956. doi:10.1016/j.cell.2005.08.020

**Brewer, J. R., Mazot, P. and Soriano, P.** (2016). Genetic insights into the mechanisms of Fgf signaling. *Genes Dev.* **30**, 751-771. doi:10.1101/gad.277137.115
**Chambers, I., Silva, J., Colby, D., Nichols, J., Nijmeijer, B., Robertson, M., Vrana, J., Jones, K., Grotewold, L. and Smith, A.** (2007). Nanog safeguards pluripotency and mediates germline development. *Nature* **450**, 1230-1234. doi:10.1038/nature06403
**Chazaud, C., Yamanaka, Y., Pawson, T., Rossant, J., He, J., Martin, W. D., Hamilton, T. C., Lambeth, J. D., Xu, X. X., Rossant, J. et al.** (2006). Early lineage segregation between epiblast and primitive endoderm in mouse blastocysts through the Grb2-MAPK pathway. *Dev. Cell* **10**, 615-624. doi:10.1016/j.devcel.2006.02.020
**Christoforou, A., Mulvey, C. M., Breckels, L. M., Geladaki, A., Hurrell, T., Hayward, P. C., Naake, T., Gatto, L., Viner, R., Arias, A. M. et al.** (2016). A draft map of the mouse pluripotent stem cell spatial proteome. *Nat. Commun.* **7**, 8992. doi:10.1038/ncomms9992
**Chu, Y., Solski, P. A., Khosravi-Far, R., Der, C. J. and Kelly, K.** (1996). The mitogen-activated protein kinase phosphatases PAC1, MKP-1, and MKP-2 have unique substrate specificities and reduced activity in vivo toward the ERK2 sevenmaker mutation. *J. Biol. Chem.* **271**, 6497-6501. doi:10.1074/jbc.271.11.6497
**Corson, L. B., Yamanaka, Y., Lai, K.-M. V. and Rossant, J.** (2003). Spatial and temporal patterns of ERK signaling during mouse embryogenesis. *Dev. Camb. Engl.* **130**, 4527-4537. doi:10.1242/dev.00669
**Deathridge, J., Antolović, V., Parsons, M. and Chubb, J. R.** (2019). Live imaging of ERK signalling dynamics in differentiating mouse embryonic stem cells. *Dev. Camb. Engl.* **146**, dev172940. doi:10.1242/dev.172940
**Ding, W., Bellusci, S., Shi, W. and Warburton, D.** (2003). Functional analysis of the human Sprouty2 gene promoter. *Gene* **322**, 175-185. doi:10.1016/j.gene.2003.09.004
**Eblaghie, M. C., Lunn, J. S., Dickinson, R. J., Münsterberg, A. E., Sanz-Ezquerro, J.-J., Farrell, E. R., Mathers, J., Keyse, S. M., Storey, K. and Tickle, C.** (2003). Negative feedback regulation of FGF signaling levels by Pyst1/MKP3 in chick embryos. *Curr. Biol.* **13**, 1009-1018. doi:10.1016/S0960-9822(03)00381-6
**Ekerot, M., Stavridis, M. P., Delavaine, L., Mitchell, M. P., Staples, C., Owens, D. M., Keenan, I. D., Dickinson, R. J., Storey, K. G. and Keyse, S. M.** (2008). Negative-feedback regulation of FGF signalling by DUSP6/MKP-3 is driven by ERK1/2 and mediated by Ets factor binding to a conserved site within the DUSP6/MKP-3 gene promoter. *Biochem. J.* **412**, 287-298. doi:10.1042/BJ20071512
**Ema, M., Mori, D., Niwa, H., Hasegawa, Y., Yamanaka, Y., Hitoshi, S., Mimura, J., Kawabe, Y., Hosoya, T., Morita, M. et al.** (2008). Krüppel-like factor 5 is essential for blastocyst development and the normal self-renewal of mouse ESCs. *Cell Stem Cell* **3**, 555-567. doi:10.1016/j.stem.2008.09.003
**Feldman, B., Poueymirou, W., Papaioannou, V. E., DeChiara, T. M. and Goldfarb, M.** (1995). Requirement of FGF-4 for postimplantation mouse development. *Science* **267**, 246-249. doi:10.1126/science.7809630
**Frankenberg, S., Gerbe, F., Bessonnard, S., Belville, C., Pouchin, P., Bardot, O. and Chazaud, C.** (2011). Primitive endoderm differentiates via a three-step mechanism involving Nanog and RTK signaling. *Dev. Cell* **21**, 1005-1013. doi:10.1016/j.devcel.2011.10.019
**Gao, Y., Liu, X., Tang, B., Li, C., Kou, Z., Li, L., Liu, W., Wu, Y., Kou, X., Li, J. et al.** (2017). Protein expression landscape of mouse embryos during pre-implantation development. *Cell Rep.* **21**, 3957-3969. doi:10.1016/j.celrep.2017.11.111
**Gasnier, M., Dennis, C., Vaurs-Barrière, C. and Chazaud, C.** (2013). Fluorescent mRNA labeling through cytoplasmic FISH. *Nat. Protoc.* **8**, 2538-2547. doi:10.1038/nprot.2013.160
**Guo, G., Huss, M., Tong, G. Q., Wang, C., Li Sun, L., Clarke, N. D. and Robson, P.** (2010). Resolution of cell fate decisions revealed by single-cell gene expression analysis from zygote to blastocyst. *Dev. Cell* **18**, 675-685. doi:10.1016/j.devcel.2010.02.012
**Hacohen, N., Kramer, S., Sutherland, D., Hiromi, Y. and Krasnow, M. A.** (1998). sprouty encodes a novel antagonist of FGF signaling that patterns apical branching of the drosophila airways. *Cell* **92**, 253-263. doi:10.1016/S0092-8674(00)80919-8
**Hamilton, W. B. and Brickman, J. M.** (2014). Erk signaling suppresses embryonic stem cell self-renewal to specify endoderm. *Cell Rep.* **9**, 2056-2070. doi:10.1016/j.celrep.2014.11.032
**Herriges, J. C., Verheyden, J. M., Zhang, Z., Sui, P., Zhang, Y., Anderson, M. J., Swing, D. A., Zhang, Y., Lewandoski, M. and Sun, X.** (2015). FGF-regulated ETV transcription factors control FGF-SHH feedback loop in lung branching. *Dev. Cell* **35**, 322-332. doi:10.1016/j.devcel.2015.10.006
**Kalkan, T., Olova, N., Roode, M., Mulas, C., Lee, H. J., Nett, I., Marks, H., Walker, R., Stunnenberg, H. G., Lilley, K. S. et al.** (2017). Tracking the embryonic stem cell transition from ground state pluripotency. *Dev. Camb. Engl.* **144**, 1221-1234. doi:10.1242/dev.142711
**Kang, M., Piliszek, A., Artus, J. and Hadjantonakis, A.-K.** (2013). FGF4 is required for lineage restriction and salt-and-pepper distribution of primitive endoderm factors but not their initial expression in the mouse. *Dev. Camb. Engl.* **140**, 267-279. doi:10.1242/dev.084996
**Kang, M., Garg, V. and Hadjantonakis, A.-K.** (2017). Lineage establishment and progression within the inner cell mass of the mouse blastocyst requires FGFR1 and FGFR2. *Dev. Cell* **41**, 496-510.e5. doi:10.1016/j.devcel.2017.05.003
**Krawchuk, D., Honma-Yamanaka, N., Anani, S. and Yamanaka, Y.** (2013). FGF4 is a limiting factor controlling the proportions of primitive endoderm and epiblast in the ICM of the mouse blastocyst. *Dev. Biol.* **384**, 65-71. doi:10.1016/j.ydbio.2013.09.023
**Kunath, T., Saba-El-Leil, M. K., Almousailleakh, M., Wray, J., Meloche, S. and Smith, A.** (2007). FGF stimulation of the Erk1/2 signalling cascade triggers transition of pluripotent embryonic stem cells from self-renewal to lineage commitment. *Dev. Camb. Engl.* **134**, 2895-2902. doi:10.1242/dev.02880
**Kurimoto, K., Yabuta, Y., Ohinata, Y., Ono, Y., Uno, K. D., Yamada, R. G., Ueda, H. R. and Saitou, M.** (2006). An improved single-cell cDNA amplification method for efficient high-density oligonucleotide microarray analysis. *Nucleic Acids Res.* **34**, e42. doi:10.1093/nar/gkl050
**Lemmon, M. A. and Schlessinger, J.** (2010). Cell signaling by receptor tyrosine kinases. *Cell* **141**, 1117-1134. doi:10.1016/j.cell.2010.06.011
**Liu, Y., Jiang, H., Crawford, H. C. and Hogan, B. L. M.** (2003). Role for ETS domain transcription factors Pea3/Erm in mouse lung development. *Dev. Biol.* **261**, 10-24. doi:10.1016/S0012-1606(03)00359-2
**Loh, Y.-H., Wu, Q., Chew, J.-L., Vega, V. B., Zhang, W., Chen, X., Bourque, G., George, J., Leong, B., Liu, J. et al.** (2006). The Oct4 and Nanog transcription network regulates pluripotency in mouse embryonic stem cells. *Nat. Genet.* **38**, 431-440. doi:10.1038/ng1760
**Marenda, D. R., Vrailas, A. D., Rodrigues, A. B., Cook, S., Powers, M. A., Lorenzen, J. A., Perkins, L. A. and Moses, K.** (2006). MAP kinase subcellular localization controls both pattern and proliferation in the developing Drosophila wing. *Dev. Camb. Engl.* **133**, 43-51. doi:10.1242/dev.02168
**Menchero, S., Rayon, T., Andreu, M. J. and Manzanares, M.** (2016). Signaling pathways in mammalian preimplantation development: Linking cellular phenotypes to lineage decisions. *Dev. Dyn.* **246**, 245-261. doi:10.1002/dvdy.24471
**Michailovici, I., Harrington, H. A., Azogui, H. H., Yahalom-Ronen, Y., Plotnikov, A., Ching, S., Stumpf, M. P. H., Klein, O. D., Seger, R. and Tzahor, E.** (2014). Nuclear to cytoplasmic shuttling of ERK promotes differentiation of muscle stem/progenitor cells. *Dev. Camb. Engl.* **141**, 2611-2620. doi:10.1242/dev.107078
**Mitsui, K., Tokuzawa, Y., Itoh, H., Segawa, K., Murakami, M., Takahashi, K., Maruyama, M., Maeda, M. and Yamanaka, S.** (2003). The homeoprotein Nanog is required for maintenance of pluripotency in mouse epiblast and ES cells. *Cell* **113**, 631-642. doi:10.1016/S0092-8674(03)00393-3
**Molotkov, A., Mazot, P., Brewer, J. R., Cinalli, R. M. and Soriano, P.** (2017). Distinct requirements for FGFR1 and FGFR2 in primitive endoderm development and exit from pluripotency. *Dev. Cell* **26**, 469-482. doi:10.1016/j.devcel.2017.05.004
**Morgani, S. M., Saiz, N., Garg, V., Raina, D., Simon, C. S., Kang, M., Arias, A. M., Nichols, J., Schröter, C. and Hadjantonakis, A.-K.** (2018). A Sprouty4 reporter to monitor FGF/ERK signaling activity in ESCs and mice. *Dev. Biol.* **441**, 104-126. doi:10.1016/j.ydbio.2018.06.017
**Mühl, B., Hägele, J., Tasdogan, A., Loula, P., Schuh, K. and Bundschu, K.** (2015). SPREDs (Sprouty related proteins with EVH1 domain) promote self-renewal and inhibit mesodermal differentiation in murine embryonic stem cells. *Dev. Dyn. Off. Publ. Am. Assoc. Anat.* **244**, 591-606. doi:10.1002/dvdy.24261
**Murakami, K., Günesdogan, U., Zylicz, J. J., Tang, W. W. C., Sengupta, R., Kobayashi, T., Kim, S., Butler, R., Dietmann, S. and Surani, M. A.** (2016). NANOG alone induces germ cells in primed epiblast in vitro by activation of enhancers. *Nature* **529**, 403-407. doi:10.1038/nature16480
**Nagy, A.** (2003). *Manipulating the Mouse Embryo: A Laboratory Manual*. Cold Spring Harbor Laboratory Press.
**Neben, C. L., Lo, M., Jura, N. and Klein, O. D.** (2017). Feedback regulation of RTK signaling in development. *Dev. Biol.* **447**, 71-89. doi:10.1016/j.ydbio.2017.10.017
**Nett, I. R., Mulas, C., Gatto, L., Lilley, K. S. and Smith, A.** (2018). Negative feedback via RSK modulates Erk-dependent progression from naïve pluripotency. *EMBO Rep.* **19**, e45642. doi:10.15252/embr.201745642
**Nichols, J., Silva, J., Roode, M. and Smith, A.** (2009). Suppression of Erk signalling promotes ground state pluripotency in the mouse embryo. *Dev. Camb. Engl.* **136**, 3215-3222. doi:10.1242/dev.038893
**Nishioka, N., Inoue, K., Adachi, K., Kiyonari, H., Ota, M., Ralston, A., Yabuta, N., Hirahara, S., Stephenson, R. O., Ogonuki, N. et al.** (2009). The Hippo signaling pathway components Lats and Yap pattern Tead4 activity to distinguish mouse trophectoderm from inner cell mass. *Dev. Cell* **16**, 398-410. doi:10.1016/j.devcel.2009.02.003
**Niwa, Y., Masamizu, Y., Liu, T., Nakayama, R., Deng, C.-X. and Kageyama, R.** (2007). The initiation and propagation of Hes7 oscillation are cooperatively regulated by Fgf and notch signaling in the somite segmentation clock. *Dev. Cell* **13**, 298-304. doi:10.1016/j.devcel.2007.07.013
**Ohnishi, Y., Huber, W., Tsumura, A., Kang, M., Xenopoulos, P., Kurimoto, K., Oleś, A. K., Araúzo-Bravo, M. J., Saitou, M., Hadjantonakis, A.-K. et al.** (2014). Cell-to-cell expression variability followed by signal reinforcement progressively segregates early mouse lineages. *Nat. Cell Biol.* **16**, 27-37. doi:10.1038/ncb2881
**Patel, A. L. and Shvartsman, S. Y.** (2018). Outstanding questions in developmental ERK signaling. *Dev. Camb. Engl.* **145**, dev143818. doi:10.1242/dev.143818
**Plusa, B., Piliszek, A., Frankenberg, S., Artus, J. and Hadjantonakis, A.-K.** (2008). Distinct sequential cell behaviours direct primitive endoderm formation in

the mouse blastocyst. *Dev. Camb. Engl.* **135**, 3081-3091. doi:10.1242/dev.021519

**Posfai, E., Petropoulos, S., de Barros, F. R. O., Schell, J. P., Jurisica, I., Sandberg, R., Lanner, F. and Rossant, J.** (2017). Position- and hippo signaling-dependent plasticity during lineage segregation in the early mouse embryo. *eLife* **6**, 1-3. doi:10.7554/eLife.22906

**Raible, F. and Brand, M.** (2001). Tight transcriptional control of the ETS domain factors Erm and Pea3 by Fgf signaling during early zebrafish development. *Mech. Dev.* **107**, 105-117. doi:10.1016/S0925-4773(01)00456-7

**Reginensi, A., Clarkson, M., Neirijnck, Y., Lu, B., Ohyama, T., Groves, A. K., Sock, E., Wegner, M., Costantini, F., Chaboissier, M.-C. et al.** (2011). SOX9 controls epithelial branching by activating RET effector genes during kidney development. *Hum. Mol. Genet.* **20**, 1143-1153. doi:10.1093/hmg/ddq558

**Roehl, H. and Nüsslein-Volhard, C.** (2001). Zebrafish pea3 and erm are general targets of FGF8 signaling. *Curr. Biol.* **11**, 503-507. doi:10.1016/S0960-9822(01)00143-9

**Saiz, N., Williams, K. M., Seshan, V. E. and Hadjantonakis, A. K.** (2016). Asynchronous fate decisions by single cells collectively ensure consistent lineage composition in the mouse blastocyst. *Nat. Commun.* **7**, 13463. doi:10.1038/ncomms13463

**Schröter, C., Rué, P., Mackenzie, J. P. and Martinez Arias, A.** (2015). FGF/MAPK signaling sets the switching threshold of a bis circuit controlling cell fate decisions in embryonic stem cells. *Dev. Camb. Engl.* **142**, 4205-4216. doi:10.1242/dev.127530

**Shapiro, P. S., Vaisberg, E., Hunt, A. J., Tolwinski, N. S., Whalen, A. M., McIntosh, J. R. and Ahn, N. G.** (1998). Activation of the MKK/ERK pathway during somatic cell mitosis: direct interactions of active ERK with kinetochores and regulation of the mitotic 3F3/2 phosphoantigen. *J. Cell Biol.* **142**, 1533-1545. doi:10.1083/jcb.142.6.1533

**Sharrocks, A. D.** (2001). The ETS-domain transcription factor family. *Nat. Rev. Mol. Cell Biol.* **2**, 827-837. doi:10.1038/35099076

**Smith, A.** (2017). Formative pluripotency: the executive phase in a developmental continuum. *Dev. Camb. Engl.* **144**, 365-373. doi:10.1242/dev.142679

**Sodhi, C. P., Li, J. and Duncan, S. A.** (2006). Generation of mice harbouring a conditional loss-of-function allele of Gata6. *BMC Dev. Biol.* **6**, 19. doi:10.1186/1471-213X-6-19

**Stavridis, M. P., Collins, B. J. and Storey, K. G.** (2010). Retinoic acid orchestrates fibroblast growth factor signalling to drive embryonic stem cell differentiation. *Dev. Camb. Engl.* **137**, 881-890. doi:10.1242/dev.043117

**Sun, X., Mariani, F. V. and Martin, G. R.** (2002). Functions of FGF signalling from the apical ectodermal ridge in limb development. *Nature* **418**, 501-508. doi:10.1038/nature00902

**Yamanaka, Y., Lanner, F. and Rossant, J.** (2010). FGF signal-dependent segregation of primitive endoderm and epiblast in the mouse blastocyst. *Dev. Camb. Engl.* **137**, 715-724. doi:10.1242/dev.043471

# Supplementary Information

## Supplementary Figure 1

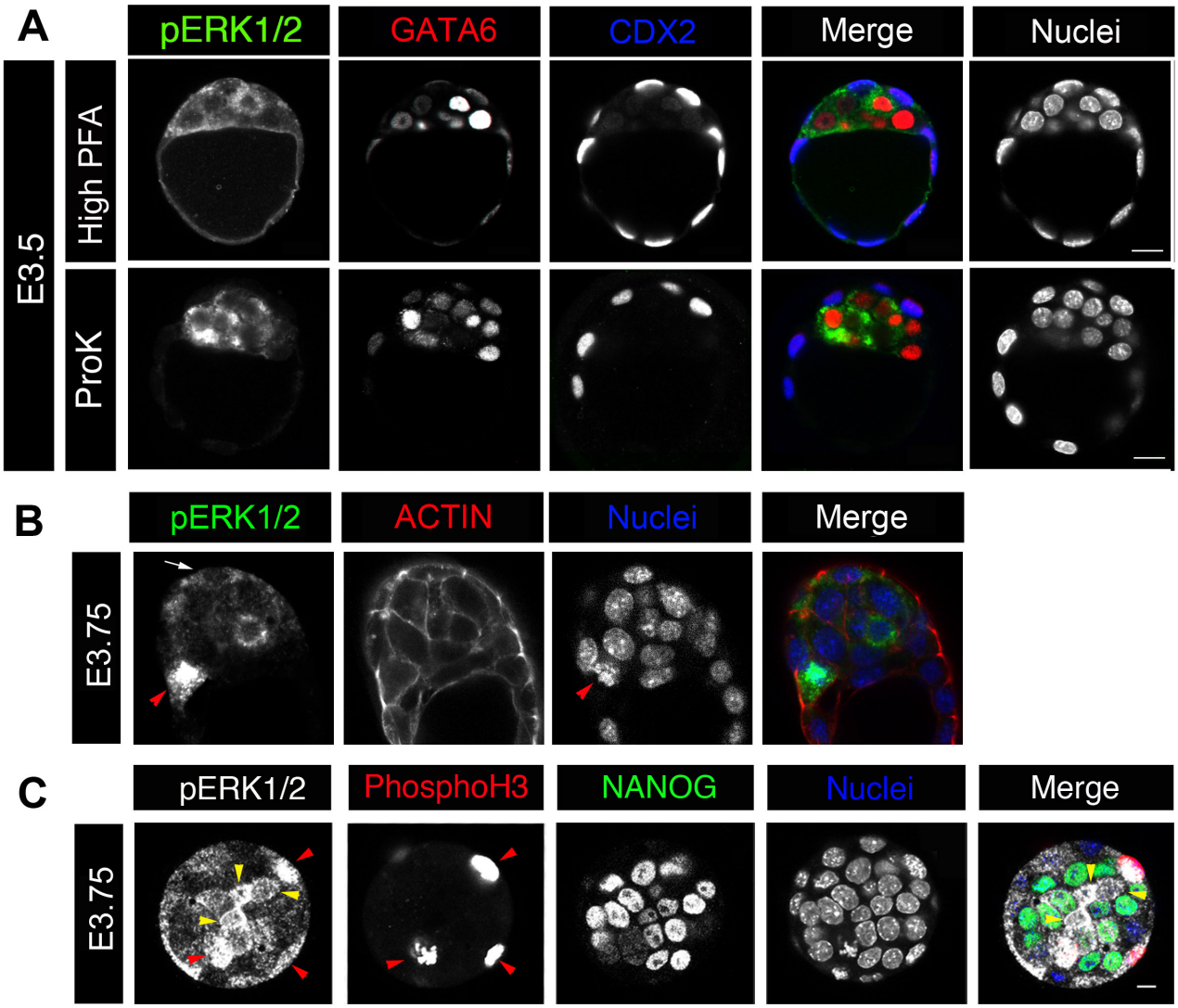


**Figure S1.** pERK labelling in blastocysts. A. Parallel staining of pERK, GATA6 and CDX2 with the High PFA and ProK protocols. B. ERK phosphorylation at E3.75 with signal in the TE (arrow) and ICM. The red arrowhead points toward a mitotic cell. C, Section through the ICM of an E3.75 embryo, stained with antibodies against pERK, NANOG and phospho-Histone3 to detect mitotic cells (n=8). Yellow arrowheads indicate cytoplasmic pERK while red arrowheads indicate nuclear pERK. Nuclear pERK cells are labelled by phospho-Histone3. Scale bars: 10 microns.

## Supplementary Figure 2

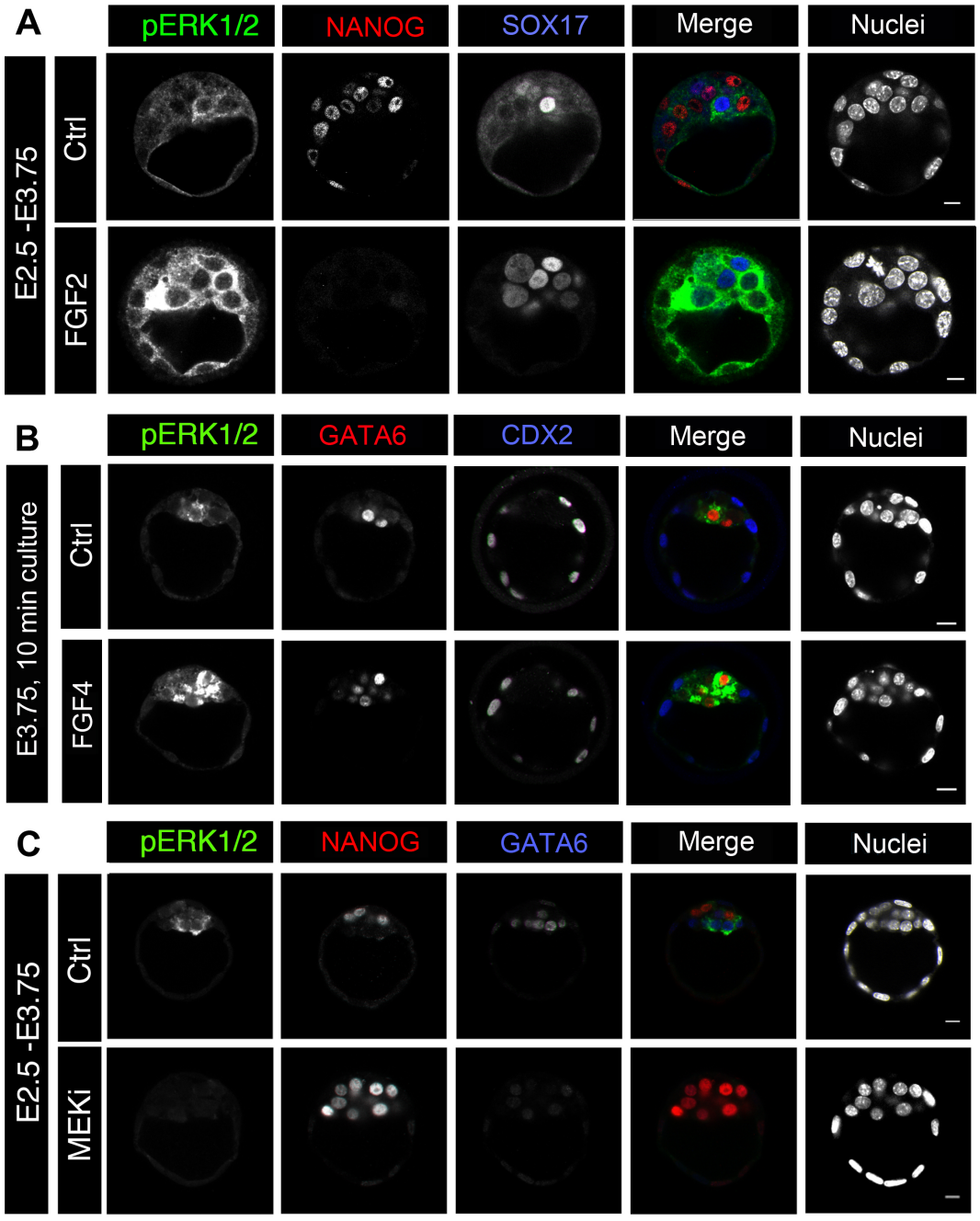


**Figure S2.** Validation of pERK staining in blastocysts. A, B. ERK phosphorylation after embryo cultures with FGF for 30h (A) (Ctrl, n=21; FGF4 n=22) or 10 min (B) (Ctrl, n=12; FGF4 n=14). C. pERK immunostaining after cultures with MEK inhibitor (Ctrl, n=18; MEK or MEK+FGFR inhibitors, n=18). Scale bars: 10 microns.

## Supplementary Figure 3

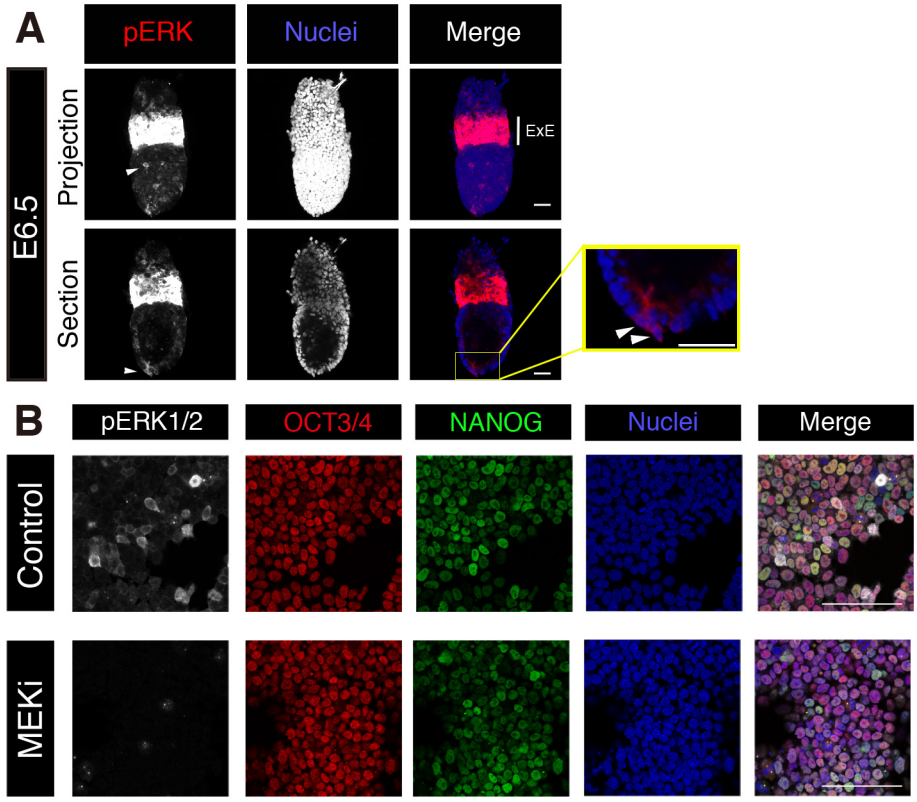


**Figure S3**: pERK immunostaining after implantation and in ES cells. **A**. ERK phosphorylation at E6.5 with a strong labelling in the extraembryonic ectoderm (ExE) and a weaker labelling in some PrE cells (arrowheads). The right panel is a magnification of the boxed area to show outside (VE) pERK-labelled cells (arrowheads). B. ERK phosphorylation in ES cells, co-stained with OCT3/4 and NANOG, cultured in absence (top panel) or presence (bottom panel) of the MEK inhibitor. Scale bars: 10 (A) and 100 (C) microns.

## Supplementary Figure 4

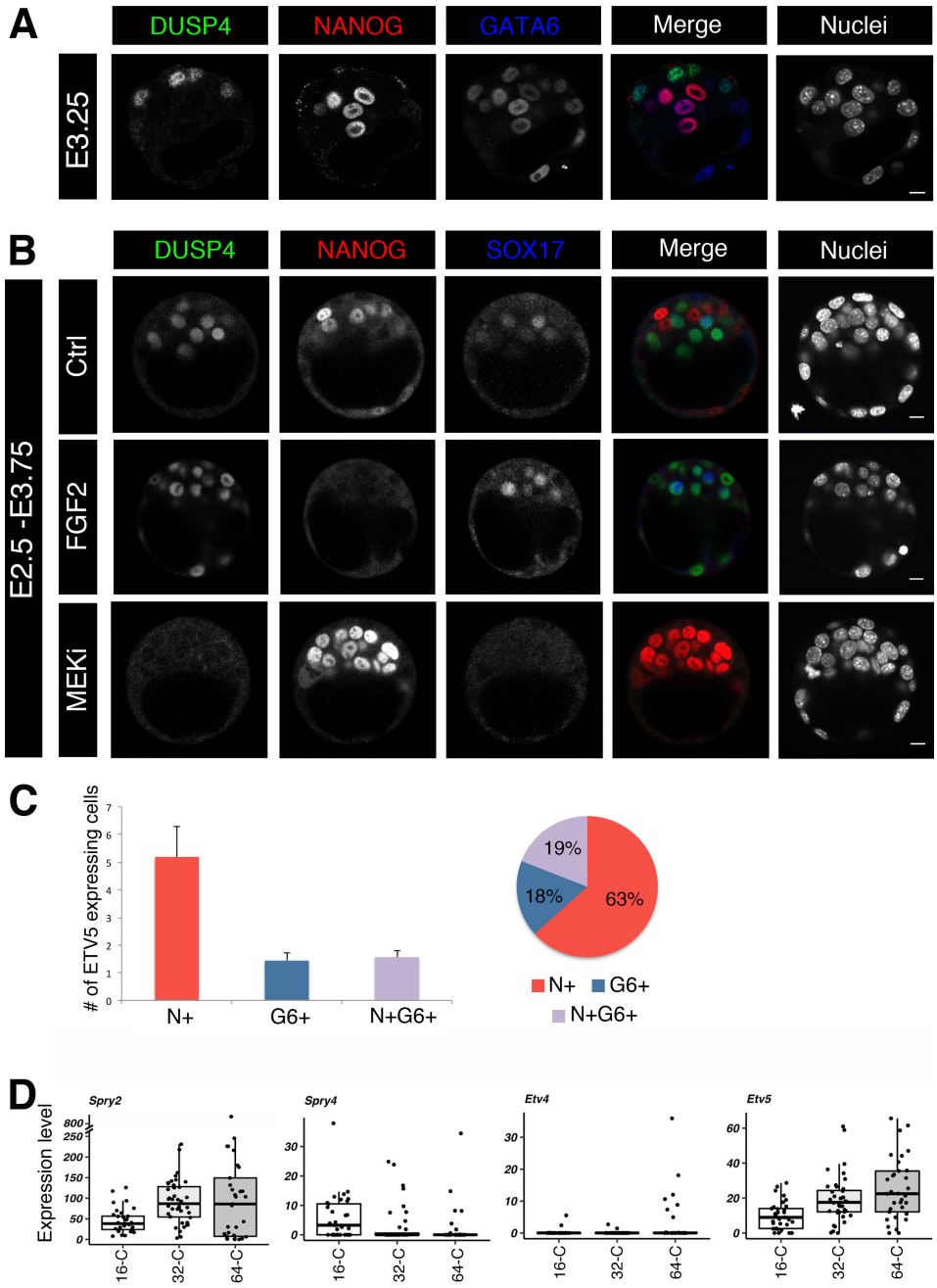


**Figure S4.** Expression of factors related to the FGF pathway. **A.** DUSP4, NANOG and GATA6 detection at E3.25 (n=15). **B**. DUSP4, NANOG and SOX17 immunolabelling in embryos cultured with either MEK inhibitor or FGF2 from E2.5 to E3.75 (Ctrl, n=20; FGF2, n= 15; MEK or MEK+FGFR inhibitors, n= 22). Scale bars: 10 microns. **C**. Number of cells labelled by ETV5 per embryo at E3.5-E3.75 (n=16 embryos) and their distribution between precursor (N+G6+), Epi (N+) or PrE cells (G6+). Data are represented as mean ± SEM. **D**. Expression of indicated genes by single-cell RNA-seq extracted from (Posfai et al., 2017) at the 16-cell stage (33 inner cells), E3.25 (32-C, 40 ICM cells) and E3.5 (64-C, 33 ICM cells). Expression levels are in RPKM.

**Table S1**: List of primary antibodies used

| Epitope | Host | Supplier | Reference | Dilution |
|---|---|---|---|---|
| pERK | rabbit | Cell Signaling | 4370 | 1/50 |
| GATA6 | goat | R&D | AF1700 | 1/300 |
| pHistone 3 | rabbit | Millipore | 06-570 | 1/100 |
| NANOG | rabbit | Abcam | ab80892 | 1/100 |
| NANOG | rat | e-bioscience | 14-5761 | 1/100 |
| DUSP4 | rabbit | Abcam | ab216576 | 1/100 |
| ETV5 | rabbit | Proteintech | 13011-1-AP | 1/100 |
| SOX17 | goat | R&D | AF1924 | 1/100 |
| CDX2 | mouse | Abcam | ab89949 | 1/1 |
| OCT3/4 | mouse | SantaCruz | Sc-5279 | 1/100 |

**Table S2**: list of primers used for the single-cell RTqPCR

| RefSeq # | Gene | Forward | Reverse |
|---|---|---|---|
| NM_176933.4 | *Dusp4* | AGCTCCTGGTTCATGGAAGC | ACTCAAAAGCCTCCTCCAGC |
| **NM_001316365** | *Etv4* | GCAGGGAAAGCTCATGGAC | GAGCCACGTCTCTTGGAAGT |
| NM_023794 | *Etv5* | CAGAACCTGGATCACAGCAA | GACTGAGGAGGGAAGGGATG |
| NM_010202 | *Fgf4* | ACTACCTGCTGGGCCTCAA | ACTCCGAAGATGCTCACCAC |
| NM_001079908 | *Fgfr1* | GCTATAACCCCAGCCACAAC | AGCCAAAGTCTGCGATCTTC |
| NM_010207 | *Fgfr2* | CACCAACTGCACCAATGAAC | GAATCGTCCCCTGAAGAACA |
| NM_001163485 | *Rpl30* | AGTCTCTGGAGTCGATCAACT | AGCCAGTGTGCATACTCTGTAG |
| NM_009092 | *Rps17* | ATGACTTCCACACCAACAAGC | GCCAACTGTAGGCTGAGTGAC |